

Quantum Manipulation of Ultracold Atoms

Academic and Research Staff

Professor Vladan Vuletic

Visiting Scientists and Research Affiliates

Dr. James K. Thompson, Dr. Vlatko Balic

Graduate Students

Yu-ju Lin, Igor Teper, Marko Cetina, Andrew Grier, Jonathan Simon, Monika Schleier-Smith, Ian Leroux, Haruka Tanji

Undergraduate Students

Huanqian Loh, Brendan Shields, Jacob Bernstein, Thaned Pruttivarasin, David Brown, YoungHyun Kim, Yiwen Chu

Support Staff

Joanna Keseberg

1. High-brightness source of narrowband, identical-photon pairs

Sponsors

National Science Foundation – Contract PHY 03-31585

The generation of photon pairs is useful for a broad range of applications, from the fundamental (exclusion of hidden-variable formulations of quantum mechanics) to the more practical (quantum cryptography and quantum computation). A key parameter determining the usefulness of a particular source is its brightness, i.e., how many photon pairs per second are generated into a particular electromagnetic mode and frequency bandwidth. Parametric down-converters based on nonlinear crystals are excellent sources of photon pairs, but typically have large bandwidths of hundreds of GHz. However, new applications are emerging that demand large pair-generation rates into the narrow bandwidths (5 MHz) suitable for strong interaction of the photons with atoms and molecules.

We have developed an atomic-ensemble source of photon pairs with spectral brightness near fundamental physical limitations and approximately three orders of magnitude greater than the best current devices based on nonlinear crystals. Unlike parametric down-converters, however, the atomic ensemble can additionally act as a quantum memory and store the second photon, allowing triggered (i.e., deterministic) generation of the second photon [1-8]. Triggered delays of up to 20 μ s have been demonstrated [8], and it is expected that optical lattices hold the potential to extend the lifetime of these quantum memories to seconds. Lastly, proposed applications in quantum information rely on joint measurements of single photons for which photon indistinguishability is crucial for high fidelity. We observe large degrees of indistinguishability in the time-resolved interference between the two generated photons.

The experimental setup consists of a laser-cooled ensemble of 10^4 Cs atoms in the TEM₀₀ mode of a low-finesse ($F=250$), single-mode optical cavity (Fig. 1). Photon pairs are generated by a four-wave mixing process that relies on quantum interference in the emission from an entangled atomic ensemble [1,9] to enhance the probability of scattering a second (read) photon into the cavity to near unity given the initial scattering of a (write) photon into the cavity (Fig. 1). Without collective enhancement, the maximum probability that the read photon would be scattered into the cavity was only 7.3×10^{-4} , and was nearly three orders of magnitude lower than the observed value of 0.57(9).

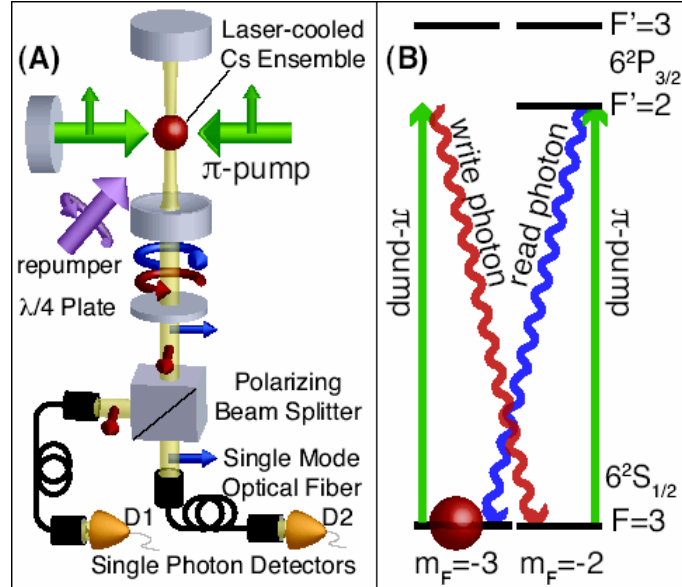


Fig. 1. (A) Experimental setup and (B) quantum states used for photon pair generation. The tuning of the π -pump laser is chosen so that the rate of write-photon scattering into the cavity is suppressed by a large detuning from resonance with any excited state, while the collectively stimulated generation of a read photon in the cavity proceeds rapidly via resonant coupling. This ensures that the time separation between subsequent pairs exceeds the time separation of the write and read photons within a pair – leading to large cross correlations between the photon polarizations. The pump and emitted-photon polarizations are denoted by the smaller arrows. The π -pump in combination with a repumper (tuned to the ground $F = 4$ to excited $F' = 4$ transition) optically pump approximately 95% of the atomic population into $|F = 3, m_F = -3\rangle$.

To first verify that the light emitted in one polarization is correlated in time with the light in the other polarization, we measure the second-order correlation function $g_{wr}(\tau)$ between the write and the read light, averaged over a bin of length T (Fig. 2). This is simply the measured coincidence count rate between the detectors D1 and D2 normalized by the rate one would expect for two completely uncorrelated beams of the same average intensities. τ specifies a time offset between the write and read windows. The time-resolved cross correlation has peak coincidence rates 100(10) times higher than for uncorrelated beams. To normalize out possible classical contributions to the cross correlation data, the autocorrelations $g_{ww}(0)$ and $g_{rr}(0)$ were also accurately measured using two detectors for each of the write and read beams. For a bin size $T = 60$ ns, the normalized cross correlation is $G = (g_{wr})^2 / (g_{ww}g_{rr}) = 760$, representing a large violation of the Cauchy-Schwarz inequality $G \leq 1$ that purely classically-correlated beams must satisfy.

To further quantify the performance of the photon-pair source, we measure the conditional probability that a read photon is emitted by the sample given that a write photon has been observed. A lower bound on this read recovery efficiency R is obtained from the measured detection losses q_r , combined with the measured probability of detecting a read photon given the detection of a write photon $R_{\text{cond}}^{\text{det}}$. The inset to Fig. 3 shows the conditional detection probability versus bin size. The integrated conditional detection probability $R_{\text{cond}}^{\text{det}} = 0.031(2)$ is estimated from the $T = 0$ intercept of a linear fit to the data at large bin size T . The read photon detection efficiency $q_r = 0.053(8)$ includes contributions from cavity mirror losses 0.45, fiber coupling 0.75, and detector quantum efficiency 0.40. Extrapolated to just outside the cavity output mirror, the recovery efficiency is $R_{\text{cond}}^{\text{cav}} = 0.26(4)$. The physical recovery efficiency for a cavity of the same linewidth, but with losses completely dominated by transmission of one of the two mirrors, is $R_{\text{cond}} = R_{\text{cond}}^{\text{det}} / q_r = 0.57(9)$. Given the low finesse $F = 250$ of the present cavity, this ideal regime could be easily achieved with current technologies.

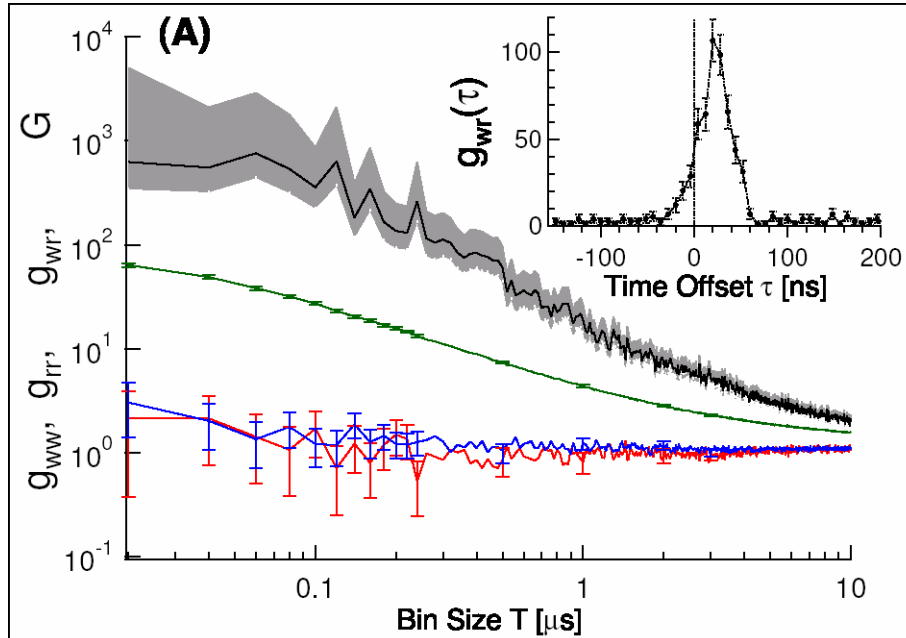


Fig. 2. Non-classical photon pair generation. (A) The measured violation of the Cauchy-Schwarz inequality $G = (g_{wr}(\tau))^2 / (g_{ww}(0)g_{rr}(0)) \leq 1$ versus bin size T (black curve with 68% confidence interval), indicating large non-classical correlations between the write and read photon beams. The inequality simply states that a cross correlation $g_{wr}(20 \text{ ns})$ (green) arising from classical sources (i.e. pump intensity fluctuations) must also manifest itself in the measured autocorrelations $g_{ww}(0)$ (red) and $g_{rr}(0)$ (blue). (inset) A time-resolved cross correlation function $g_{wr}(\tau)$ is shown with peak value 100(10).

The frequency bandwidths of the write and read photons are 1.1(2) MHz, much narrower than the 10 MHz cavity linewidth, making the photons ideal for interacting with narrowband systems such as atoms, molecules and optical cavities. By separately heterodyning the write and read photons with laser light derived from the pump laser (measured linewidth of 50 kHz), the power spectral density of the photons was obtained from the Fourier transform of the measured second-order autocorrelation function (see Fig. 3D). The photons are nearly Fourier-transform limited, as can be seen from the 2 MHz FWHM power spectrum (see Fig. 3E) of the measured cross-correlation function $g_{wr}(\tau)$ taken at slightly different parameters.

The identicalness of the write and read photons (apart from their opposite polarization) was examined via two-photon interference at the polarizing beam splitter (see Fig. 1A). This was accomplished by analyzing the write and read photons in a polarization basis rotated by 45° with respect to the usual basis used to deterministically separate the photons. Neglecting interference between the two photons, one expects that in half the cases, the photons register a coincidence count on opposite detectors. However, if the write and read photons perfectly overlap in time and frequency, there is a complete destructive interference for the probability of a coincidence count (a so-called Hong- Ou-Mandel interference [10]). The fractional reduction of the coincidence count rate below $\frac{1}{2}$ of its original value is a direct measure of the degree of indistinguishability of the photons.

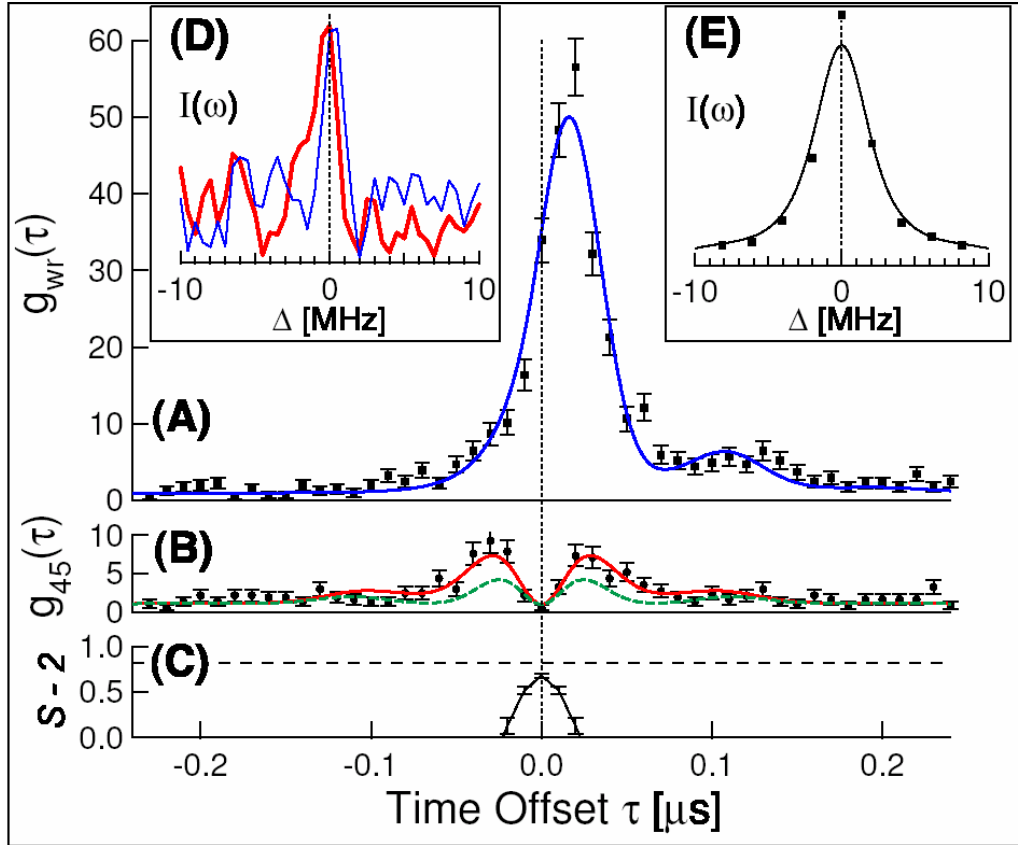


Fig. 3. Measures of identicalness and photon frequency bandwidths. (A) The time-resolved cross correlation function $g_{wr}(\tau)$ and (B) the same function $g_{45}(\tau)$ measured in a polarization basis rotated by 45° . In the 45° basis, coincidence events are suppressed by two-photon interference resulting from the near-indistinguishability of the photons. Assuming the photons have identical frequencies, the quantity $g_{45}(\tau)$ can be predicted directly from $g_{wr}(\tau)$ (green dashed curve in (B)). The prediction is more accurate if a photon frequency difference $\Delta\omega/2\pi = 2.5$ MHz is assumed (red curve in (B)). (C) The predicted violation of a Bell's inequality $S-2 < 0$ if the photon pairs were used to produce polarization-entangled photons. The dashed line is the maximum possible violation. (D) The frequency bandwidths of the write (red) and read (blue) photons are determined to be 1.1(2) MHz from the displayed heterodyne beat notes. For comparison, (E) shows the square of the Fourier transform of $(g_{wr}(\tau) - 1)^{1/2}$ taken at different parameters, indicating that the photon bandwidths are nearly transform limited.

In conclusion, we generate narrowband pairs of nearly identical photons at a rate 5×10^4 pairs/s from a laser-cooled atomic ensemble inside an optical cavity. A two-photon interference experiment demonstrates that the photons can be made 90% indistinguishable, a key requirement for quantum information processing protocols. Used as a conditional single-photon source, the system operates near the fundamental limits on recovery efficiency (57%), Fourier-transform limited bandwidth, and pair-generation-rate limited suppression of two-photon events (factor of 33 below the Poisson limit.) Each photon has a spectral width of 1.1 MHz, ideal for interacting with atomic ensembles that form the basis of proposed quantum memories and logic.

2. Resonator-aided single-atom detection on a microchip

Sponsors

DARPA

National Science Foundation – Contract PHY 03-31585

Magnetic traps and waveguides produced by microfabricated structures can trap ultracold atoms and Bose-Einstein condensates in very small volumes [11]. Preparation and detection of single atoms in microtraps could constitute an important step toward quantum information processing with neutral atoms, which could take advantage of the tight, complex, precisely controlled, and scalable magnetic traps available on microchips. In this context, the problem arises of how to detect small atom numbers in magnetic microtraps close to a substrate surface with a good signal-to-noise ratio.

Atom detection can be implemented via fluorescence or absorption methods, and resonator-aided detection is advantageous for both. For fluorescence, the resonator enhances the emission of light through the Purcell effect by a factor $2F/\pi$, where F is the cavity finesse. Similarly, the absorption of light circulating inside the resonator is enhanced by the same factor compared to a single passage through the region occupied by the atom.

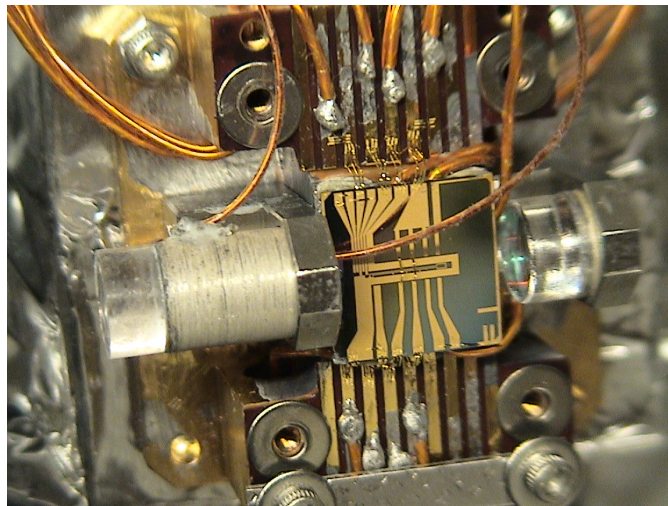


Fig. 4. Microfabricated chip with mounted optical resonator. The resonator mode is aligned $200\ \mu\text{m}$ above the surface of the microchip. The left mirror is mounted on a piezoceramic tube for tuning of the resonance frequency. The resonator finesse is $F = 8000$.

Fig. 4 shows the microfabricated chip with attached (macroscopic) optical resonator. The resonator supports a TEM_{00} mode $200\ \mu\text{m}$ above the chip surface. The resonator finesse is $F=8000$, corresponding to a photon emission probability of $\eta=13\%$ into the resonator mode. Here η is the mode cooperativity parameter for a single atom. The light exiting the resonator is delivered to a single-photon counter via a single-mode optical fiber.

We initially load 10^5 rubidium atoms into a Ioffe-Pritchard microtrap located $200\ \mu\text{m}$ from the surface, outside the cavity mode in order to prevent heating by the cavity-length stabilization light. We then use a fast radio frequency evaporation to remove all but a small number of cold atoms

at a typical temperature of 15 μK . We ramp the magnetic field to move the trap into the cavity mode, turn off the locking light, and perform the fluorescence or absorption measurement. When located in the cavity, the magnetic trap has transverse and axial vibration frequencies around 300 and 50 Hz, respectively.

For the fluorescence measurement, we illuminate the atoms with a retroreflected pump beam resonant with the D_2 line, and measure the number of photons scattered into the resonator in 250 μs . By analyzing histograms of the number of detected photons, we can extract independently the average number of atoms prepared in the trap, and the average number $\langle p \rangle$ of photon counts per atom. We find that we register $\langle p \rangle = 1.4(3)$ counts per atom, at a background count of $\langle b \rangle = 0.07$. This means that, if we set our detection threshold to ≥ 1 count, our single-atom detection is characterized by an atom quantum efficiency of 75% and a false detection rate of 7%, at a maximum single-atom count rate of 4 kHz.

While the fluorescence measurement makes a good single-atom detector, we expect an absorption measurement to provide better atom number resolution for atom numbers $a > 1$. For absorption detection, we couple the probe laser beam into the cavity TEM_{00} mode and monitor the resonant transmission through the cavity in the presence of atoms. Similarly to fluorescence detection, we compile histograms collected in 1 ms for different atom preparation parameters and fit them, assuming Poisson statistics for both the atoms and the photons per atom, to determine the mean absorption per atom $\langle s \rangle$. We find $\langle s \rangle = 3.3(3)\%$, in good agreement with the expected absorption per atom, $\langle s \rangle = 3.2(7)\%$.

Using the measured values for fluorescence and absorption, we can evaluate how well these two methods can determine the atom number in a single measurement. The expected atom number uncertainty Δa using fluorescence (absorption) detection due to both photon shot noise and the statistical uncertainty in the mean number of photons per atom $\langle p \rangle$ (uncertainty in the mean absorption per atom, $\langle s \rangle$), as well as the background photon counts (for fluorescence only), is plotted as a function of atom number in Fig. 5; the figure also includes a computed normalized histogram that characterizes the single-atom detection capability of our fluorescence measurement. For fluorescence, the atom number resolution is limited by the shot noise of the collected signal photons, which grows with atom number, while, for absorption, where the number of collected photons actually decreases with atom number, the resolution remains nearly flat, at around 1 atom [12].

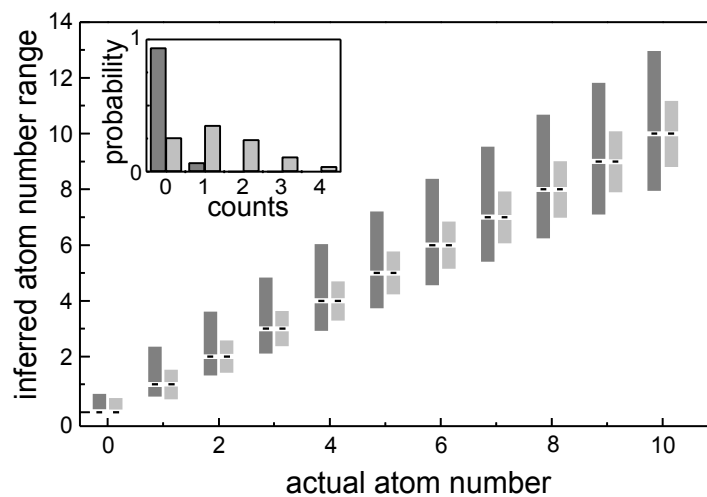


Fig. 5. Single-shot atom number measurement 1- σ confidence intervals for fluorescence (dark gray) and absorption (light gray). The inset shows computed normalized photon count distributions due to background counts (dark gray) and to photons collected from one atom (light gray) for fluorescence single-atom detection.

We also plan to use the optical resonator for the preparation of entangled states in order to improve precision experiments and atomic clocks. The best atomic clocks are now at the standard quantum limit (atomic-shot-noise limit) for which the precision scales as $1/\sqrt{N}$, where N is the number of atoms composing the clock. This is the highest precision that can be obtained with a system of independent spin- $1/2$ particles. Improved sensitivity should be attainable if one can prepare collective states where the state of one atom depends on the states of the other atoms in the sample (entangled states).

References

- [1] L.-M. Duan, M. D. Lukin, J. I. Cirac, and P. Zoller, "Generation of nonclassical photon pairs for scalable quantum communication with atomic ensembles", *Nature* **414**, 413 (2001).
- [2] Kuzmich, W. P. Bowen, A. D. Boozer, A. Boca, C. W. Chou, L.-M. Duan, and H. J. Kimble, "Generation of nonclassical photon pairs for scalable quantum communication with atomic ensembles", *Nature* **423**, 731 (2003);
- [3] H. van der Wal, M. D. Eisaman, A. Andre, R. L. Walsworth, D. F. Phillips, A. S. Zibrov, and M. D. Lukin, "Atomic Memory for Correlated Photon States", *Science* **301**, 196 (2003);
- [4] M. D. Eisaman, L. Childress, A. Andre, F. Massou, A. S. Zibrov, and M. D. Lukin, "Shaping quantum pulses of light via coherent atomic memory", *Phys. Rev. Lett.* **93**, 233602, (2004).
- [5] C. W. Chou, H. de Riedmatten, D. Felinto, S. V. Polyakov, S. J. van Enk and H. J. Kimble, "Measurement-induced entanglement for excitation stored in remote atomic ensembles", *Nature* **438**, 828 (2005).
- [6] T. Chanelière, D. N. Matsukevich, S. D. Jenkins, S.-Y. Lan, T. A. B. Kennedy and A. Kuzmich, "Storage and retrieval of single photons transmitted between remote quantum memories", *Nature* **438**, 833 (2005).
- [7] M. D. Eisaman, A. André, F. Massou, M. Fleischhauer, A. S. Zibrov and M. D. Lukin, "Electromagnetically induced transparency with tunable single-photon pulses", *Nature* **438**, 837 (2005).
- [8] D. N. Matsukevich, T. Chanelière, S. D. Jenkins, S.-Y. Lan, T. A. B. Kennedy, and A. Kuzmich, "Deterministic Single Photons via Conditional Quantum Evolution", *Phys. Rev. Lett.* **97**, 013601, (2006).
- [9] Vlatko Balic, Danielle A. Braje, Pavel Kolchin, G. Y. Yin, and S. E. Harris, "Generation of Paired Photons with Controllable Waveforms", *Phys. Rev. Lett.* **94**, 183601 (2005).
- [10] C. K. Hong, Z. Y. Ou, and L. Mandel, "Measurement of subpicosecond time intervals between two photons by interference", *Phys. Rev. Lett.* **59**, 2044 (1987).
- [11] Y. Lin, I. Teper, C. Chin, and V. Vuletic, "Impact of Casimir-Potential and Johnson Noise on Bose-Einstein Condensate Stability near Surfaces", *Phys. Rev. Lett.* **92**, 050404 (1-4) (2004).
- [12] I. Teper, Y. Lin, and V. Vuletic, "Resonator-Aided Detection of Single Atoms on a Microchip", *Phys. Rev. Lett.* **97**, 023002 (1-4) (2006).

Publications

Journal Articles

Published:

“A High-Brightness Source of Narrowband, Identical-Photon Pairs,” J. K. Thompson, J. Simon, H. Loh, and V. Vuletic, *Science* **303**, 74-77 (2006).

“Resonator-Aided Detection of Single Atoms on a Microchip,” I. Teper, Y. Lin, and V. Vuletic, *Phys. Rev. Lett.* **97**, 023002 (1-4) (2006).

“On-Demand Superradiant Conversion of Atomic Spin Gratings into Single Photons with High Efficiency,” A.T. Black, J. K. Thompson, and V. Vuletic, *Phys. Rev. Lett.* **95**, 33601 (1-4) (2005).

Submitted for publication:

“Influence of grating parameters on the linewidths of external-cavity diode lasers,” H. Loh, Y. Lin, I. Teper, M. Cetina, J. Simon, J.K. Thompson, and V. Vuletic, submitted to *Applied Optics* (March 2006).

Meeting Papers

I. Teper, Y. Lin, A.T. Black, J. Simon, J.K. Thompson, and V. Vuletic, “Single photons, single atoms, and squeezed spins,” EuroConference on Ultracold Gases and their applications, (San Feliu de Guixols, Spain, September 2005).

A.T. Black, J.K. Thompson, and V. Vuletic, “Single photons from many atoms”, IQEC/CLEO-PR2005 (Tokyo July 2005).

J.K. Thompson, J. Simon, and V. Vuletic, “Narrowband source of identical-photon pairs,” Photonics West 2006, San Jose (January 2006), talk given by J. Thompson.